Korean J. Chem. Eng., **29**(6), 804-811 (2012)
DOI: 10.1007/s11814-011-0240-0

Optimization of lead removal from aqueous solution by micellar-enhanced ultrafiltration process using Box-Behnken design

Bashir Rahmanian*, Majid Pakizeh*,†, and Abdolmajid Maskooki**

*Department of Chemical Engineering, Faculty of Engineering, Ferdowsi University of Mashhad, P. O. Box 91775-1111, Mashhad, Khorasan 9177948944, Iran
**Department of Khorasan Research Institute for Food Science and Technology (KRIFST), 12 Km., Asian Highway, Khorasan Science and Technology Park (KSTP), Mashhad, Iran
(*Received 8 May 2011 • accepted 9 September 2011*)

Abstract−The main objective of this research was to use Box-Behnken experimental design (BBD) and response surface methodology (RSM) for optimization of micellar-enhanced ultrafiltration (MEUF) to remove lead ions from synthetic wastewater using spiral-wound ultrafiltration membrane. The critical factors selected for the examination were surfactant concentration, molar ratio of surfactant to metal (S/M) and solution pH. A total of 17 experiments were accomplished towards the construction of a quadratic model for both target variables. The experimental results were fitted with a second-order polynomial equation by a multiple regression analysis, and more than 95%, 93% of the variation could be predicted by the models for lead rejection and permeation flux, respectively. The optimum condition was found by using the obtained mathematical models. Optimization indicated that in C_{SDS}=2 mM, pH=6.57 and S/M= 9.82 maximum flux and rejection efficiency can be achieved, simultaneously.

Key words: MEUF, Lead, Box-Behnken Design, Optimization

INTRODUCTION

Today, heavy metals removal is one of the major challenges in industrial wastewater treatment plants. In many industries, such as electroplating and metal industries, metal parts coating production process, acid battery manufacturing, ammunition, ceramic and glass industries, large amounts of wastewater contaminated with heavy metals such as Pb^{2+}, copper, cadmium, silver, mercury, chromium and nickel may occur. These harmful pollutants have genetic, toxic and carcinogenic effects on humans and aquatic life [1-3]. Pb^{2+} is one of the harmful metal ions found in wastewaters from various industries such as metal plating and battery plants. It is a very toxic element that can damage the nervous system, kidneys and reproductive system. Consequently, the removal of metal ions and/or organic contaminants from aqueous solutions is a problem frequently encountered in the treatment of industrial wastewaters.

There are several physical, chemical and biotechnological processes for removing of heavy metals from aqueous solution, such as adsorption, chemical precipitation, biotechnology, ion exchange and membrane separation [4-7]. The stringent environmental and ecological requirements have spurred the search for industrial waste treatment options with low energy, labor, and capital costs, but the traditional techniques for the removal of metal ions from aqueous effluents are incapable of reducing concentration to the levels required by law or are prohibitively expensive. Therefore, removal of heavy metals from large volumes of polluted water at low concentrations by traditional methods is not economical. Recently, membrane separation, due to its simple operation and convenience, has been used for a wide form of wastewater treatment containing heavy metals. Different types of membrane processes, including NF, UF, ELM and RO, are used for this purpose [8-12]. MEUF processes have been used to remove heavy metals and are an established research field for the separation of inorganic pollutants from the liquid phases [13-15]. The combination of surfactants and membranes in separation of dilute polluted water has led to the development of novel techniques or enhancement of existing techniques. In this technology, surfactants are added to the solution to promote the removal of metal ions. The surfactant molecules will aggregate and form spherical micelles. The anionic micelles, which are negatively charged, can bind to Pb^{2+} ions, which are positively charged. Then the solution can be filtered through an ultrafiltration membrane whose pore size is smaller than the micelle size to reject the micelles. At the same time, Pb^{2+} ions adsorbed onto the micelles are rejected.

Several researches have been conducted about heavy metal removal in MEUF, but few studies have been performed about lead removal by MEUF from the aqueous solutions using spiral-wound membrane.

The spiral-wound membrane element is the most widely used membrane device because it has a high membrane surface area to volume ratio, it is easy to replace and can be manufactured from a wide variety of materials [16]. Nowadays, more and more spiral-wound membranes are applied in various industries due to their advantages, such as compact structure and low cost [15,17].

The main objective of this study is to investigate the performance of MEUF process for lead removal and application of experimental design approach to find the optimum operational conditions of the proposed process. Optimization of the significant factors in the MEUF process via the conventional method of investigation involves the changing of one variable in time while all other variables are

†To whom correspondence should be addressed.
E-mail: pakizeh@um.ac.ir

fixed at constant levels, and studying the effect of the single variable on the response. This classical approach is time-consuming and complicated for a multi-variable system. To overcome such difficulty, the statistical techniques as DOE for the study of MEUF process have been applied. The experimental design used is a good mathematical tool to optimize the experimental results, verifying the validity and rapidly obtaining the optimal values for the variables. Box and Behnken (1960) proposed three-level experimental designs for fitting response surfaces. These designs are formed by combining 2^k factorials with incomplete block designs. The resulting designs are usually very efficient in terms of number of required runs, and they are either rotatable or nearly rotatable. This statistical design was used in the current study to determine the quantitative relationship between the response and the levels of the experimental factors. Subsequently, optimization of those levels was carried out [18].

MATERIALS AND METHODS

1. Chemicals

99% purity of sodium dodecyl sulfate (SDS, molecular weight of 288.38 and critical micelle concentration (cmc) 8.15 mM) was purchased from Merck Ltd, Germany. Lead (II) acetate (Pb $(CH_3COO)_2$ with molecular weight of 379.34) with purity of 99% was obtained from Merck company. The surfactant was used without any further treatment. All the solutions were prepared using distilled water.

2. Apparatus and Procedure

The schematic view of experimental set-up is in Fig. 1. In this system, a spiral-wound membrane made of regenerated cellulose acetate with an effective area of 1.83 m^2 and MWCO of 10 kD (PL series, Millipore) was used.

Regenerated cellulose is the cellulose membrane of choice and is both purer and more chemical resistant than cellulose acetate or mixed cellulose esters. This type of polymer has good solvent resistance and is able to work over a wide pH range [14,15]. A peristaltic pump to provide the required pressure and flow was used. All experiments were conducted in 25 °C (room temperature) to prevent any deposition. Desired aqueous solution was prepared by adding certain amounts of lead acetate in distilled water. The solution was continuously stirred with a mixing speed of 300 rpm. After each series of experiments was completed, UF membrane was flushed and backwashed with distilled water and cleaned with 0.1 N NaOH and 0.01 N HCl. The backwashing was performed for 15 min and distilled water was circulated until the pH of the permeate flux became neutral. Before each run, ultrapure water was filtered in order to determine the permeability and to check the membrane.

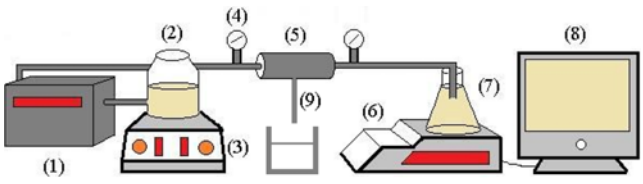

Fig. 1. Schematic of micellar-enhanced ultrafiltration process.

1. Peristaltic pump
2. Feed reservoir
3. Magnetic stirrer
4. Monometer
5. Spiral-wound ultrafiltration module
6. Balance
7. Permeate stream reservoir
8. Computer in which data of permeate weight are registered
9. Retentate stream

Feed solution volume was 500 cm^3 and operation was continued until the permeate volume exceeded 200 cm^3. Permeate flux was measured continuously and the flux data saved in an excel file by the flow program. Pb^{2+} concentration was measured using atomic absorption (GBC, 908AA model) with a wavelength of 288.8 nm. Samples of MEUF were pretreated according to the standard method.

The transmembrane pressure (TMP) can be calculated by Eq. (1):

$$\Delta P = \frac{P_f + P_r}{2} - P_p \tag{1}$$

In this equation, P_r, P_f and P_p are retentate pressure, feed pressure and permeate pressure (it is almost insignificant), respectively. Permeate flux of ultrafiltration was calculated as follows:

$$J_p = \frac{Q}{A.\Delta t} \tag{2}$$

Where J_p, Q, t and A are permeate flux (mL/m^2·s), collected permeate volume (mL), permeate collection time (sec) and effective surface of membrane (m^2), respectively. Lead removal efficiency was calculated using Eq. (3):

$$R\% = \left(1 - \frac{C_p}{C_f}\right) * 100 \tag{3}$$

where R % is rejection efficiency, C_p and C_f are concentration of Pb^{2+} in feed and permeate streams, respectively.

RESULTS AND DISCUSSION

1. Design of Experiments and Response Surface Modeling

The main advantage of experimental design is that it covers a larger area of experimental statistics and obtains unambiguous results at minimum expense. With fractional factorial design methodology, the main and interaction effects can be easily evaluated. The main effect refers to the effect caused by the changed factor, while the interaction effect refers to when the effect of one factor is dependent on the value of another factor. Recently, design of experiments and response surface methodology (RSM) have been proven to be effective tools for investigation, modeling and optimization of the enhanced ultrafiltration processes [19].

The Box-Behnken design used for the modeling of micellar-enhanced ultrafiltration process was carried out by choosing three factors (design variables): SDS concentration (C_{SDS}, mM), molar ratio of SDS concentration to Pb^{2+} ion concentration (S/M) and pH of

Table 1. Design variables and their coded and actual values for experimental design

Factor	Level		
	−1	0	+1
A: SDS concentration in feed (mM)	2	4	6
B: Solution pH	2	7	12
C: Molar ratio of SDS concentration to lead ion concentration (S/M)	5	10	15

feed solution. The operating ranges and the levels of the considered variables are given in Table 1. Each factor at two levels (high (+1) and low (−1)) and the center point (coded level 0), which is the midpoint between the high and low levels, is repeated five times.

The results of two responses, rejection efficiency R (%) and permeate flux (mL/m^2·s), were determined experimentally according to designed runs in order to ascertain the performance of the complex process. Generally, a second-order polynomial response for three variables is a quadratic model as:

$$Y = \beta_0 + \sum_{i=1}^{k} \beta_i x_i + \sum_{i=1}^{k} \beta_{ii} x_i^2 + \sum_{i<j} \beta_{ij} x_i x_j \quad (4)$$

where Y represents the predicted responses, x_i and x_j are the coded values of independent variables, β_0 is the intercept coefficient, β_i are the linear coefficients, β_{ii} are the squared coefficients, and β_{ij} are the interaction coefficients.

2. Analysis of Variance (ANOVA)

The significance of Box-Behnken design was tested by means of analysis of variance (ANOVA). The sum of squares used to estimate the effect of the factors and the F distribution, which is the distribution of the ratio of respective mean-square effect and mean-square error, are shown in Tables 2 and 3. Having the F-value and the degree of freedoms, the P-value is then calculated. The smaller the p-value, the more evidence we have against the null hypothesis. Most investigators accept the model for prediction if the P-value is less than 0.05 [18]. The ANOVA shows that the model source of

Table 2. Analysis of variance (ANOVA) for RSM (response: rejection efficiency)

Source	Sum of Squares	df	Mean Square	F Value	P-value Prob > F	
Model	5247.31	7	749.62	27.58	0.0001<	Significant
A-C_{sds}	455.11	1	455.11	16.75	0.0027	
B-S/M	0.55	1	0.55	0.020	0.8904	
C-pH	114.53	1	114.53	4.21	0.0703	
AC	141.73	1	141.73	5.22	0.0473	
BC	212.87	1	212.87	7.83	0.0208	
B^2	66.10	1	66.10	2.43	0.1533	
C^2	4184.64	1	4184.64	153.98	0.0001<	
Residual	244.59	9	27.18			
Lack of fit	115.39	5	23.08	0.71	0.6453	Not significant
Pure error	129.20	4	32.30			
Cor total	5491.89	16				
Std. Dev.	5.21		R-squared	0.9555		
Mean	72.38		Adj R-squared	0.9208		
C.V. %	7.20		Pred R-squared	0.8319		
PRESS	923.41		Adeq precision	14.156		

Table 3. Analysis of variance (ANOVA) for RSM (response: permeate flux (mL/m^2·min))

Source	Sum of Squares	df	Mean Square	F Value	P-value Prob>F	
Model	11.60	6	1.93	22.91	<0.0001	Significant
A-Csds	3.26	1	3.26	38.66	<0.0001	
B-S/M	2.40	1	2.40	28.40	0.0003	
C-pH	0.59	1	0.59	6.97	0.0247	
AB	0.48	1	0.48	5.72	0.0378	
BC	1.05	1	1.05	12.44	0.0055	
B^2	3.82	1	3.82	45.24	<0.0001	
Residual	0.84	10	0.084			
Lack of fit	0.15	6	0.026	0.15	0.9789	Not significant
Pure error	0.69	4	0.17			
Cor total	12.45	16				
Std. Dev.	0.29	R-squared	0.9322			
Mean	7.69	Adj R-squared	0.8915			
C.V. %	3.78	Pred R-squared	0.8718			
PRESS	1.60	Adeq precision	18.199			

variability has been subdivided into several components. The terms A and A^2 are the linear and quadratic effects of SDS concentration, B and B^2 are linear and quadratic effect of S/M ratio and C and C^2 are the linear and quadratic effects of pH. The terms AB, BC and AC represent linear*linear components of the 3-factor interaction. An F test is displayed for the model source of variation. As shown in Table 2, the p-value is small (<0.0001), so the interpretation of this test is that the model is significant.

The fitted models were assessed with the coefficient of determination, R^2. A concern with this statistic is that it always increases as terms are added to the model, even though the added terms are often not significant. Consequently, this statistic is usually smaller for the refined model in comparison with corresponding full model. To negate this drawback, the adjusted coefficient of determination, R^2-Adj. is used. This statistic is adjusted to the size of the model, more specifically, the number of factors. The addition of nonsignificant terms to the model can usually decrease the R^2 Adj. value. As shown in Table 2, the R-squared calculated for rejection efficiency is 0.9555, reasonably close to 1, which is acceptable. It implies that about 95.55% of the variability in the data is explained by the model. The predicted R^2 (0.8319) is agreement with the adjusted coefficient of determination R^2 adj. (0.9208). The lack-of-fit P-value of 0.6453 showed that the lack of fit was not important relative to the pure error. The lack-of-fit can also be said to be insignificant. This is desirable as we want a model that fits. The larger the *t*-value and the smaller the *p*-value, the more significant is the corresponding coefficient. Thus, the ranking of significant parameters in this study was as follows: C^2>A>BC>AC>C>B^2>B. To improve the effect of significant parameters, the insignificant parameters were eliminated and the final equation in terms of coded factors is shown in Eq. (5):

$$R\% = +89.06 + 7.54*A + 0.26*B + 3.78*C + 5.95*AC - 7.30*BC - 3.96*B^2 - 31.48*C^2 \quad (5)$$

The same procedure is applied on the other response variable; permeate flux and the resulting ANOVA table are shown in Table 3.

In this case, the F-value (22.91) is also clearly departing from unity and p-value is <0.0001.The R-squared for permeate flux is 0.9322 and R^2 Adj. is 0.8915, close to 1, which is desirable. The P-values of the factor A, B, C, AB, BC and C^2 present the relatively higher statistical significance to other interactions. While, the AC, C^2 and A^2 interactions were not significant with high P-values. The second-order RSM with coded variables are as follows:

$$\text{Permeate Flux} = 8.13 - 0.64*A - 0.55*B - 0.27*C - 0.35*AB - 0.51*BC - 0.95*B^2 \quad (6)$$

To judge if the selected model provides adequate approximation of the real system or not, the statistical plots were provided by the Design Expert 8.0.4 software. Fig. 2 shows the normal probability plots of the studentized residuals (e), which may be defined by Eq. (7) for any observation as the difference between the experimental (y_{exp}) and predicted response ($\hat{y}_{predic.}$), for Pb^{2+} rejection efficiency and permeate flux.

$$e = y_{exp} - \hat{y}_{predic.} \quad (7)$$

The general impression from examining this display is that the error distribution is approximately normal, and it is clear from the figure

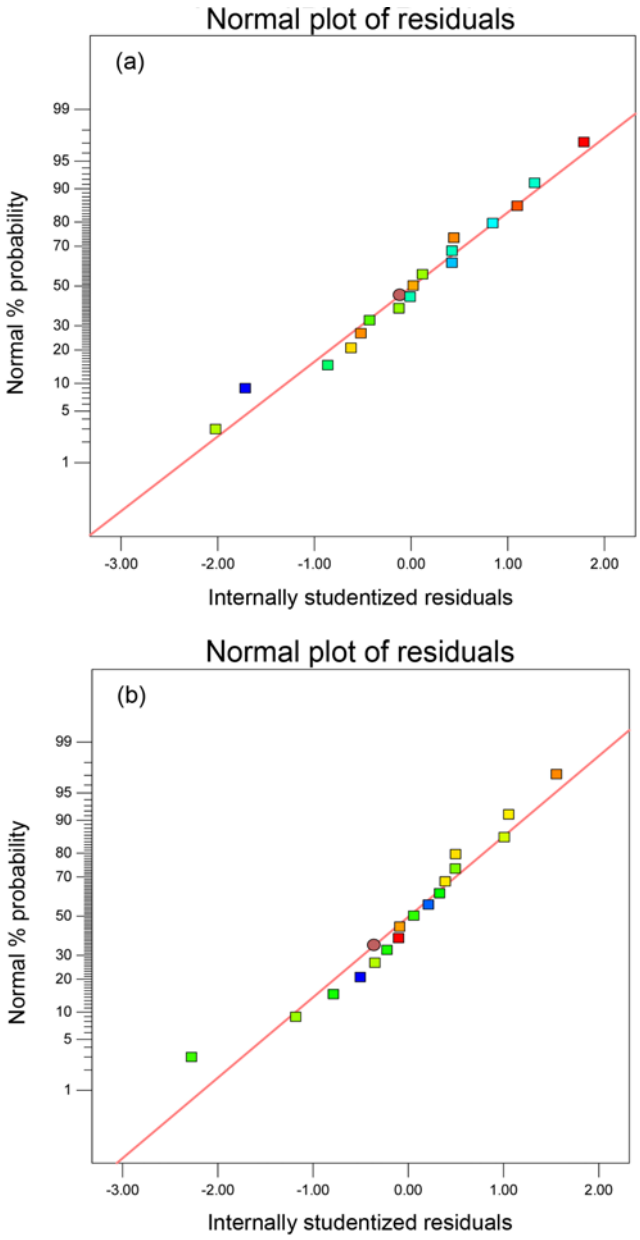

Fig. 2. Normal probability plot of residual for (a) rejection efficiency and (b) permeate flux.

that the residuals follow a straight line. The tendency of the normal probability plot to upward slightly on left side in Fig. 2(b) implies that the tail of the error distribution is somewhat thinner than would be anticipated in a normal distribution; however, this plot is not grossly nonnormal. All of the standardized residuals should fall within ±3. A residual bigger than three standard deviations from zero is a potential outlier. The normal probability plots in Fig. 2 give no indication of outliers.

If the model is correct and assumptions are satisfied, the residuals should be structureless; in particular, they should be unrelated to any other variable including the predicted response. A simple check is to plot the residuals versus the fitted values $\hat{y}_{predic.}$. Fig. 3 plots the residuals versus the fitted values of the rejection efficiency (a) and permeate flux (b). Fig. 3(a) shows a distinct pattern

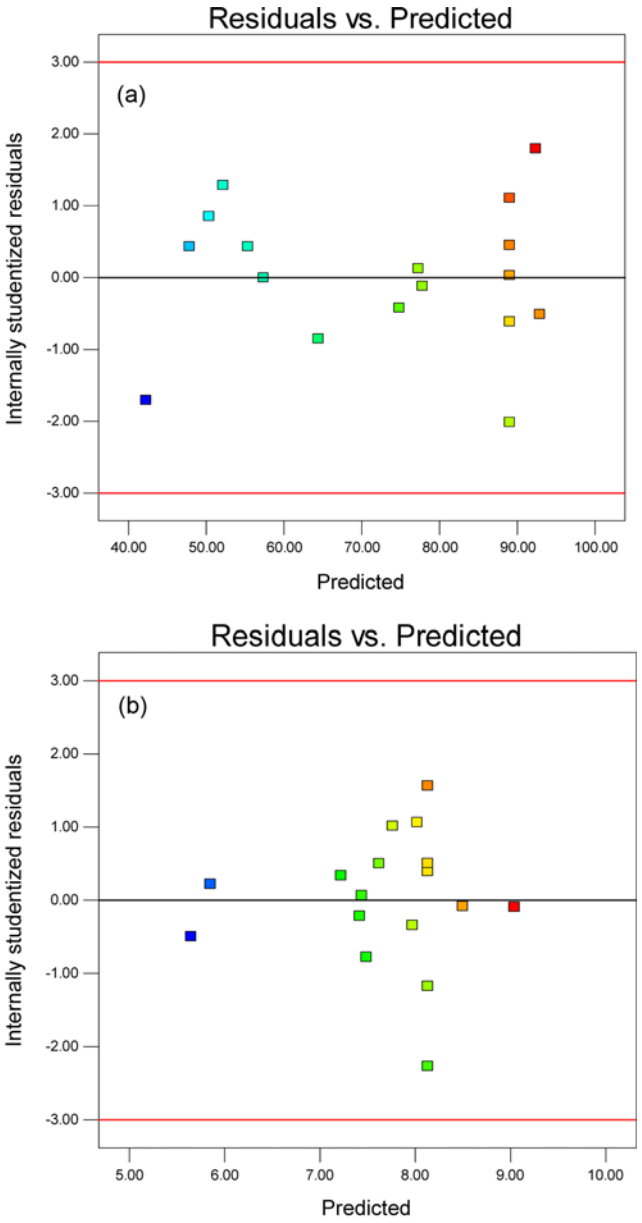

Fig. 3. Plot of residual vs. predicted response for (a) rejection efficiency and (b) permeate flux.

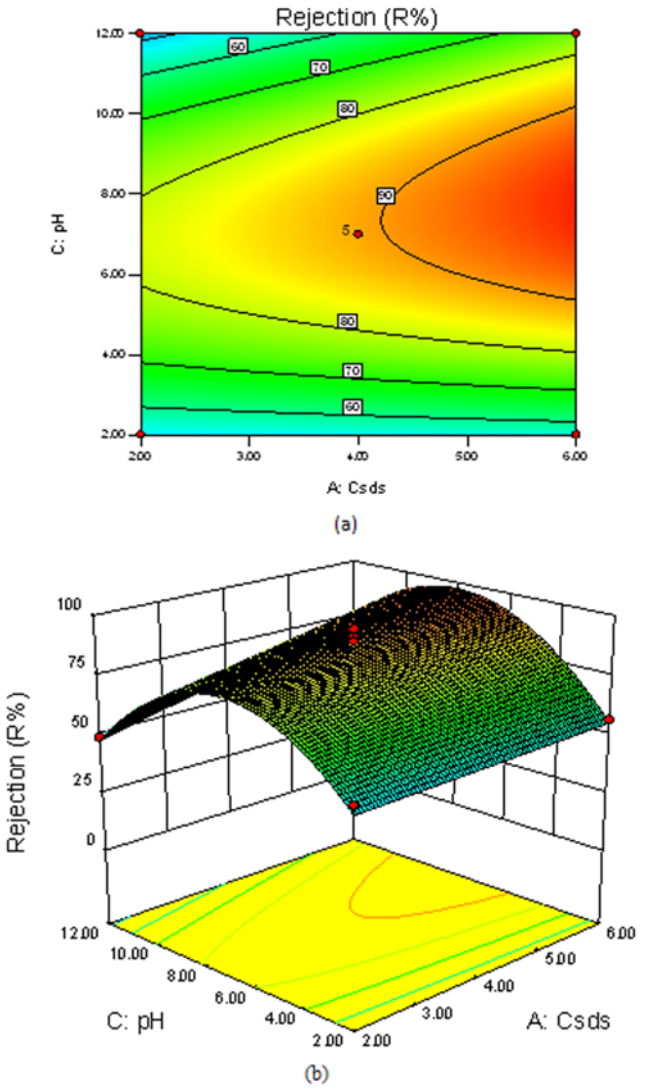

Fig. 4. Response surface and contour plots showing the effective parameters; pH and SDS concentration as well as their mutual effect on the Pb^{2+} rejection while other parameters was kept constant at middle level (S/M=10).

move from negative to positive to negative to positive to negative to positive again. This structure is the result of interaction between SDS concentration and pH. In Fig. 3(b) there is some mild tendency for the variance of residuals to increase as the permeate flux increases. The problem, however, is not severe enough to have a dramatic impact on the analysis, so this response was accepted as legitimate.

3. Effect of Selected Factors on pb^{2+} Rejection Efficiency

In the Figs. 4-7, the 3D surface response plots and contour-lines map of the quadratic model are presented for both responses: rejection efficiency and permeate flux. Fig. 4 shows the effect of pH and SDS concentration at constant S/M ratio of 10. The maximum response zone for Pb^{2+} reduction is observed at pH of 4 and SDS concentration higher than 4 mM. The rejection of Pb^{2+} ions was increased with increasing surfactant concentration below the cmc because the number of micelles increased with increasing nonionic surfactant concentration, which enhanced the surfactant rejection and rejection of Pb^{2+} ions solubilized in the micelles of surfactants. From Fig. 4, it can be seen that suggested range of pH values was within about 6.5-7.5.

Fig. 5 shows the changing of the S/M level from 5 to 15 and pH increasing from 2 to 12 at constant SDS concentration of 4 mM. It illustrates that the increasing of pH to 7 will enhance Pb^{2+} rejection efficiency from 60% to 90%, while the effect of S/M factor is negligible. Thus the operation should be done at high pH because H^+ can be bound to the micelles and occupies the binding sites. Accordingly, the Pb^{2+} rejection efficiency decreases with the decrease of pH. From examination of the contour plot, we note that the process may be slightly more sensitive to changes in pH than to changes in S/M. The optimum is near pH=7 and S/M=10.

4. Effect of Selected Factors on Permeate Flux

In spite of the many advantages of ultrafiltration, flux decline

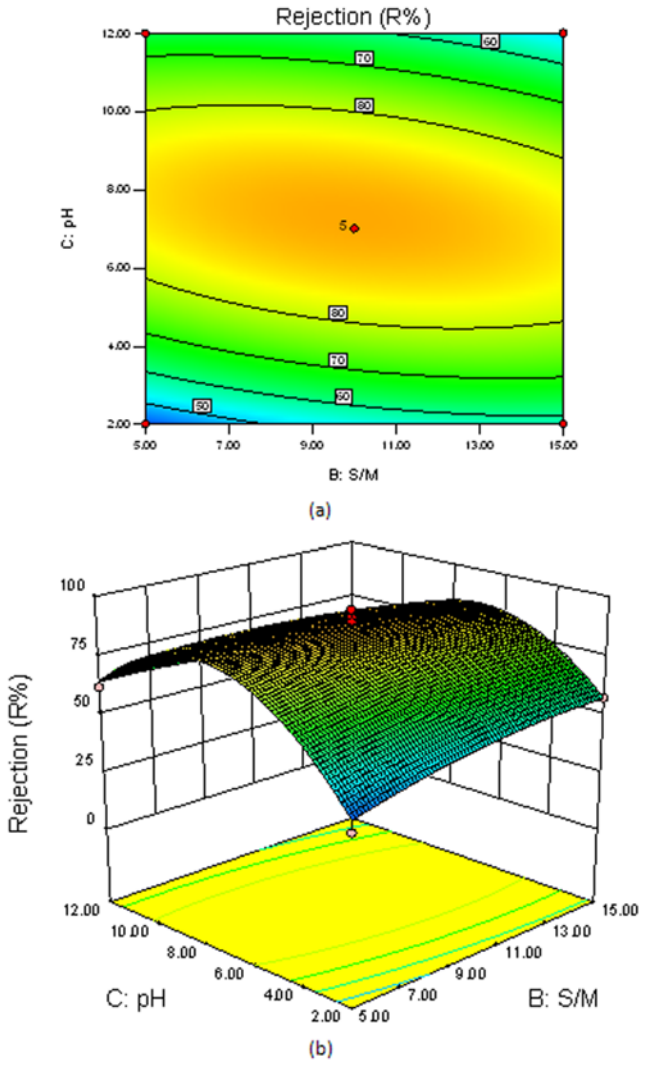

Fig. 5. Response surface and contour plots showing the effective parameters; pH and S/M ratio as well as their mutual effect on the Pb^{2+} rejection while other parameters was kept constant at middle level (C_{SDS}=4).

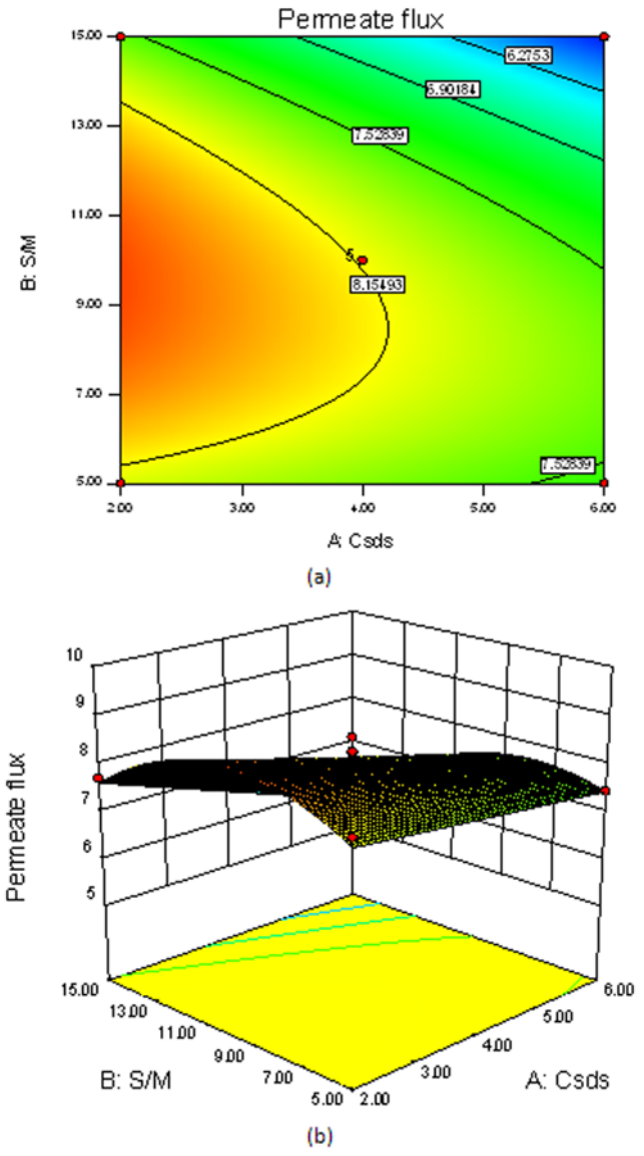

Fig. 6. Response surface and contour plots showing the effective parameters; S/M ratio and SDS concentration as well as their mutual effect on the permeate flux while other parameters was kept constant at middle level (pH=7).

remains the most serious and inherent obstacle for the efficient application of membrane separation process. Flux decline is caused by several factors such as concentration polarization, fouling, adsorption of surfactant, gel layer formation, and pore plugging. Therefore, not only the separation efficiency of Pb^{2+} ions and the optimization of process variables but also the flux behavior in surfactant-based ultrafiltration should be investigated systematically.

Fig. 6 shows the three-dimensional response surface plot and the contour plot for the permeate flux response in term of the variables SDS concentration and S/M ratio at pH 7. It is relatively easy to see from examining this figure that the permeation flux decreases from 8 to 6 with the increase of the SDS concentration from 2 to 6 mM, below cmc, because the concentration polarization has an important effect on the permeation flux. This effect can cause a resistance against the permeation. When the SDS concentration reaches and exceeds the CMC, many micelles form in the solution to block the membrane pores [20]. The optimum is near a C_{SDS} of 2 mM and S/M ratio of 10 that the response is at maximum at this point.

It can be seen from Fig. 7 that the pH effect on the permeate flux is negligible, while increasing of S/M ratio up to 10 causes decreasing the permeate flux at 4 mM constant concentration of SDS. It is clear in Fig. 7 that varying S/M ratio from 5 to 15 causes decreasing flux from 8 to 6. At higher S/M ratio, more micelles were accumulated on the membrane surface, reducing the driving force and consequently lowering the permeate flux. There could have been another possibility for the partial blockage of membrane pores by micelles and a formation of an additional resistant layer which may have decreased the flux. From examination of the plots, the maximum flux is achieved at S/M ratio of 6.

5. Optimization of Operational Conditions

Experimental optimization approach based on RSM method was used to determine the feasible optimal point. The results concerning optimal point found are reported in Table 4. Optimization of

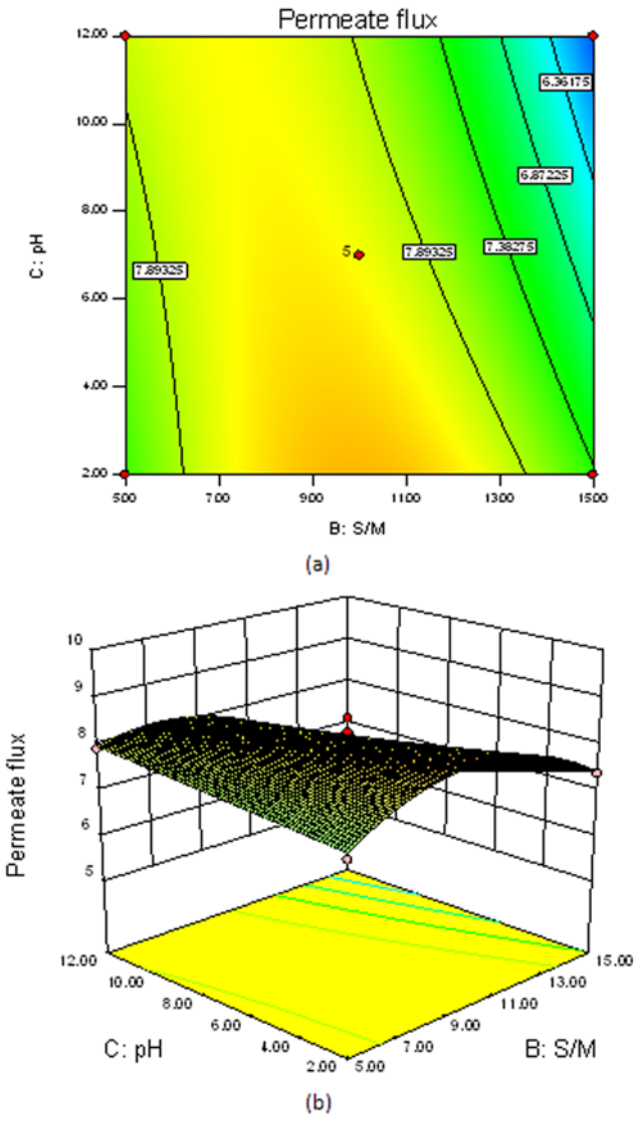

Fig. 7. Response surface and contour plots showing the effective parameters; S/M ratio andpH as well as their mutual effect on the permeate flux while other parameters was kept constant at middle level (C_{SDS}=4).

the factors levels was carried out by minimizing the amount of C_{SDS} and S/M ratio, and maximizing the rejection efficiency (optimum result 1), permeate flux (optimum result 2) and both responses together (optimum result 3). The optimal process conditions determined by RSM method are as follows: C_{SDS}=6 mM, S/M=9.39 and pH 7.84, in such conditions the rejection efficiency of 99.47% was obtained. This value (R=99.47%) is the highest rejection efficiency value obtained in all experiments conducted in this work (result 1). It is clear in Table 4 that the value of 9.04 was obtained for maximum permeate flux at pH=2.21, S/M=10.82 and C_{SDS}=2.05 mM (result 2). The optimal experimental conditions for both responses simultaneously that ensure a rejection efficiency of 81.43% and permeate flux of 8.88 (mL/m^2·s) were determined at pH=6.57, S/M=9.82 and C_{SDS}=2 mM (result 3).

Finally, a comparison between this study and previous works for Pb^{2+} removal using membrane processes is shown in Table 5. It can be observed that ELM separation [15] has a higher removal efficiency, but this type of membrane process has inherent problems, including low amount of separation and not economical. MEUF processing gives high removal efficiency and high permeate flux. The MEUF process in this study using spiral-wound membrane (R%=99.41) has proven to be more efficient when compared to flat polyethersulfone membrane (R%=98.4) [11]. As shown in this table, the Pb^{2+} rejection efficiency was at maximum 81% in the NF process [21], while the MEUF process showed higher than 99% rejection efficiency. In addition, this method has other advantages, such as simple operation and lower energy consumption than other membrane separation processes, such as NF. Also, it can be said that other enhanced ultrafiltration such as polymer enhanced ultrafiltration [22] showed less rejection efficiency (99%) compared this study.

CONCLUSION

A statistical experimental design was applied for the investigation and response surface modeling of micellar-enhanced ultrafiltration process for lead removal from aqueous solution using SDS as surfactant. The RSM method was statistically validated by ANOVA and used for prediction of rejection efficiency and permeates flux.

Table 4. Optimization results for the percentage of rejection and permeate flux for pb^{2+} removal

Optimum result	C_{SDS} (mM)	S/M	pH	Rejection (R %)	Permeate flux (mL/m^2·min)	Desirability
1	6	9.39	7.84	99.47	------	0.968
2	2.05	10.82	2.21	-------	9.04	1
3	2	9.82	6.57	81.43	8.88	0.85

Table 5. Maximum of lead rejection at this study and previous works

Type of process	Membrane material	Module type	Initial Pb^{2+} concentration (mg/L)	Maximum Pb^{2+} rejection	Ref.
ELM	(W/O/W)	NA	400-1000	99.5	[10]
MEUF	Polyethersulfone	Flat	20	98.4	[11]
PEUF	Inner ceramic	Tubular	25	99	[16]
NF	Polyamide	Tubular	100-1600	81	[17]
Present study	Regenerated cellulose acetate	Spiral-wound	50-150	99.41	

It was found that the SDS concentration and S/M ratio have major effects on permeate flux, while pH has no significant effect. Also, the results indicated that feed pH, SDS concentration and S/M ratio have effects on Pb^{2+} rejection. Optimization by RSM methodology shows the maximum Pb^{2+} rejection efficiency of 99.47% was obtained at pH=7.84, S/M=9.39 and C_{SDS}=6 mM.

ACKNOWLEDGEMENTS

The authors are indebted to the Department of Khorasan Research Institute for Food Science and Technology (KRIFST), Khorasan Science and Technology Park (KSTP), Mashhad, Iran for their financial assistance and support.

NOMENCLATURE

Symbol

R : filtration efficiency
C_p : concentration of Pb^{2+} in the feed solution [mM]
C_f : concentration of Pb^{2+} in the permeate [mg/L]
P_i : inlet pressure [bar]
P_o : outlet pressure [bar]
P_p : permeate pressure [bar]
Q : permeate volume [mL]
A : area of membrane [m^2]
Jp : permeation flux [$mL/m^2 \cdot s$]

Abbreviations

MEUF : micellar-enhanced ultrafiltration
CMC : critical micellar concentration
ANOVA : analysis of the variance
RSM : response surface methodology
TMP : transmembrane pressure [bar]
BBD : box-behnken design
ELM : emulsion liquid membrane
PEUF : polymer enhanced ultrafiltration
NF : nanofiltration

REFERENCES

1. F. R. Spellman, *Handbook of water and wastewater treatment plant operations*, Lewis Publishers Technology & Engineering (2003).
2. Patterson, William, J. *Industrial wastewater treatment technology*, Butterworth (1985).
3. M. Sánchez, *Causes and effects of heavy metal pollution*, Nova Science Publishers Inc. New York (2008).
4. H. T. Odum, *Heavy metals in the environment*, Lewis Publishers, Science (2000).
5. T. A. Kurniawan, G. Y. S. Chan, W. H. Loa and S. Babel, *Chem. Eng. J.*, **118**, 83 (2006).
6. T. Bahadir, G. Bakan, L. Altas and H. Buyukgungor, *Enzyme Microb. Technol.*, **41**, 98 (2007).
7. L. Hajiaghababaei, A. Badiei, M. R. Ganjali, S. Heydari, Y. Khaniani and Gh. Mohammadi Ziarani, *Desalination*, **266**, 182 (2011).
8. M. Cheryan, *Ultrafiltration and Microfiltration Handbook*, University of Illinois, Urbana, Illinois (1998).
9. Ch. W. Li, Y. M. Liang and Y. M. Chen, *Sep. Purif. Technol.*, **45**, 213 (2005).
10. R. Sabry, A. Hafez and M. Khedr, *Desalination*, **212**, 165 (2007).
11. P. Yenphan, A. Chanachai and R. Jiraratananon, *Desalination*, **253**, 30 (2010).
12. G. Son and S. Lee, *Korean J. Chem. Eng.*, **28**, 793 (2011).
13. B. Rahmanian, M. Pakizeha and A. Maskooki, *J. Hazard. Mater.*, **184**, 261 (2010).
14. B. Rahmanian, M. Pakizeh, S. A. A. Mansoori and R. Abedini, *J. Hazard. Mater.*, **187**, 67 (2011).
15. B. Rahmanian, M. Pakizeh, M. Esfandyari, F. Heshmatnezhada and A. Maskooki, *J. Hazard. Mater.*, **192**, 585 (2011).
16. A. Bodalo-Santoyo, J. L. Gomez-Carrasco, E. Gomez-Gomez, M. F. Maximo-Martin and A. M. Hidalgo-Montesinos, *Desalination*, **160**, 151 (2004).
17. B. Rahmanian, M. Pakizeh, M. Esfandyari and A. Maskooki, *Sep. Sci. Technol.*, **46**, 1571 (2011).
18. D. C. Montgomery, *Design and analysis of experiments*, 7th Ed. (2009).
19. D. J. Wheeler, *Understanding industrial experimentation*, 2nd Ed. (2006).
20. F. Ferella, M. Prisciandaro, I. D. Michelis and F. Veglio, *Desalination*, **207**, 125 (2007).
21. S. Bouranene, P. Fievet, A. Szymczyk, M. El-Hadi Samar and A. Vidonne, *J. Membr. Sci.*, **325**, 150 (2008).
22. P. Canizares, A. Perez, R. Camarillo and R. Mazarro, *J. Membr. Sci.*, **320**, 520 (2008).